Analytical Damage Assessment of Prestressed Concrete Containment Vessels Behaviour under Blast Induced Fire Loading

Seung Jai Choi[1*], Tae Hee Lee[2], Joon Hee Park[3], Soo Ho Han[4], Jang Ho Jay Kim[5]

[1*] *School of Civil and Environmental Engineering, Yonsei University, Yonsei-ro 50, Seodaemun-gu, Seoul 03722, South Korea*
(seungjaechoi@yonsei.ac.kr)
[2] *School of Civil and Environmental Engineering, Yonsei University, Yonsei-ro 50, Seodaemun-gu, Seoul 03722, South Korea*
(saintlth@yonsei.ac.kr)
[3] *School of Civil and Environmental Engineering, Yonsei University, Yonsei-ro 50, Seodaemun-gu, Seoul 03722, South Korea*
(sdc03208@naver.com)
[4] *School of Civil and Environmental Engineering, Yonsei University, Yonsei-ro 50, Seodaemun-gu, Seoul 03722, South Korea*
(skyblueway96@naver.com)
[4] *School of Civil and Environmental Engineering, Yonsei University, Yonsei-ro 50, Seodaemun-gu, Seoul 03722, South Korea*
(jjhkim@yonsei.ac.kr)

Abstract

Recently, explosions, collisions, and fires have occurred frequently around the world due to terror attacks, and impact accidents. Particularly, since the 9.11 terror attack, public anxiety heightened due to lack of safety in our society. The incidents can be viewed as examples of possible extreme loading scenarios that can occur in structures and infrastructures. Among all of structures and infrastructures, prestressed concrete containment vessels (PCCVs) are the most vulnerable structures from terrors and accidents. Therefore, in this study, finite element simulation program of LS-DYNA and MIDAS FEA, are used to evaluate of PCCVs applied with blast induced fire loading resistance. Since the blast test on a full-scale PCCV is not realistically possible, it is necessary to develop a precise simulation tool to accurately evaluate the damage level of a full-scale PCCV. This study aims to improve the accuracy of the simulation tool by calibrating simulation programs using model test data. Then, the parametric study is conducted according to the explosive charge weight, standoff distance, and concrete compressive strength of a PCCV using calibrated blast and fire simulation tools. Based on the study results, the level of damage assessment to PCCVs applied with blast-fire loading can be precisely evaluated.

Keywords: Blast loads; Fire resistance; Infrastructure; Simulation; Damage assessment

1. Introduction

In recent years, explosions, collisions, and fires have occurred frequently around the world due to terror attacks, impact accidents, and human hazards. Particularly, since the 9.11 terror attack on the World Trade Center and the Pentagon of the United States in 2001, public anxiety heightened due to lack of safety in our society. The incidents can be viewed as representative examples of possible extreme loading scenarios that can occur in structures and infrastructures. Among all of structures and infrastructures, prestressed concrete containment vessels (PCCVs) and liquefied natural gas (LNG) storage tanks are the most vulnerable structures from terrors and accidents. Public fear of nuclear accidents from nuclear containment vessel damages, which have great physical and environmental consequences drastically increased since the Fukushima Daiichi nuclear disaster in 2011.

Generally, PCCV and LNG storage tanks are constructed as bi-directional prestressed concrete (PSC) shell structure. Because of the vulnerability of these containment structures under extreme loading scenarios, various studies on physical and structural safety of PSC structures from extreme loading conditions have been conducted by researchers all over the world [1-4]. Protective Design Center (PDC) of the US Army Corps of Engineers conducted blast researches on the structural

behaviors subjected to blast loads to develop ConWEP program for calculating blast pressures from bomb explosions and a simple single degree of freedom simulation program SBEBD for designing of protective structures in the 1990s. Based on these research results, TM5-1300 technical manual was published to establish disaster preventive technology for concrete structures and to implement these technologies in the design. Under the supervision of the US Nuclear Regulatory Commission (NRC), Sandia National Laboratory of the US constructed a 1/6 and 1/4 scale model of a RC and PSC reactor containment structure, respectively, to experimentally evaluate their behaviors at extreme load [1]. Ross et al. (1997) experimentally evaluated the behavior of beams and slabs applied with ANFO explosive loads to determine the explosion resistance performance of concrete members [5]. Muszynski et al. (2003) experimentally evaluated blast behavior of RC members by applying explosive pressure to various reinforced concrete wall structures [6]. However, due to national security reasons, only small portion of blast study results are disclosed publically. Because of lack of published study results on the topic, no clear standards or specifications in the form of design codes for civil structures related blast loading are available presently. Therefore, this study aims to predict the damage levels of real scale PCCVs from blast and fire loading by simulations to propose disaster preventive measures of the structural details of PCCVs.

2. Blast Induced Fire Test for Bi-directional Prestressed Concrete Panels

Since the full scale blast tests on actual PCCV structure is not realistically possible, it is necessary to develop a precise simulation tool to obtain the accurate results to evaluate the damage level of full-scale PCCV structures. This study aims to improve the accuracy of the simulation tool by calibrating simulation programs using experimental data. High strain rate appropriate constitutive models, load conversion technique, spalling implementation technique, prestressing applying technique, etc. are used to improve the simulation accuracies. Blast tests are performed on scaled down bi-directional PCCV wall model to obtain data needed for the calibration. Blast charge of ANFO 55lbs and fire load curve of RABT curve are used for the blast-fire combined loading tests. The test specimens consisted of reinforced concrete (RC), prestressed concrete without reinforcing bar (PSC), and prestressed concrete with reinforcing bar (PSRC) panels. Also, the experimental data for fire loaded PSC panels are compared to the simulation results to verify the thermal failure behavior. For the simulation of blast loaded PCCV, a commercial explicit finite element program LS-DYNA is used. For the simulation of fire loaded PCCV, a commercial implicit finite element program MIDAS FEA is used. The precision simulation results are verified by the experimental data of blast, fire, and blast-fire combined loading. Then, full-scale structural simulations of PCCV applied with blast and fire loadings are conducted using LS-DYNA and MIDAS FEA to evaluate damage levels of PCCV structure, followed by parametric study to propose disaster preventive measures of the structural details of PCCVs.

2.1 Target PCCV details

APR-1400 (Advanced Power Reactor 1400) PCCV, the next generation PCCV for Korean nuclear power plant, is selected as the target structure for the blast test in this study. Since the outer wall of a PCCV is designed and constructed as a bi-directional prestressed concrete (PSC) member, the bi-directional PSC panel is chosen as a specimen type. The PCCV design of APR-1400 is shown in Fig 1(a). Based on the PS tendon arrangement in a standard PCCV outer wall as shown in Fig. 1(b), the tendon arrangement of the APR-1400 PCCV is assumed. In a standard PCCV, PS tendon layout is in two directions (vertical and meridional) for the outer wall and three arcs with an angle difference of 120° for the roof dome. The wall has three or four buttresses for post-tensioned tendon anchorages. In the outer wall, it is structurally advantageous to place PS tendons inside of the outer reinforcing bars, the vertical tendons to pass through the center of the wall, and the meridional tendons placement toward outer surface of the wall. Based on the basic guidelines described above, the target specimen is modeled to be compatible to the design details.

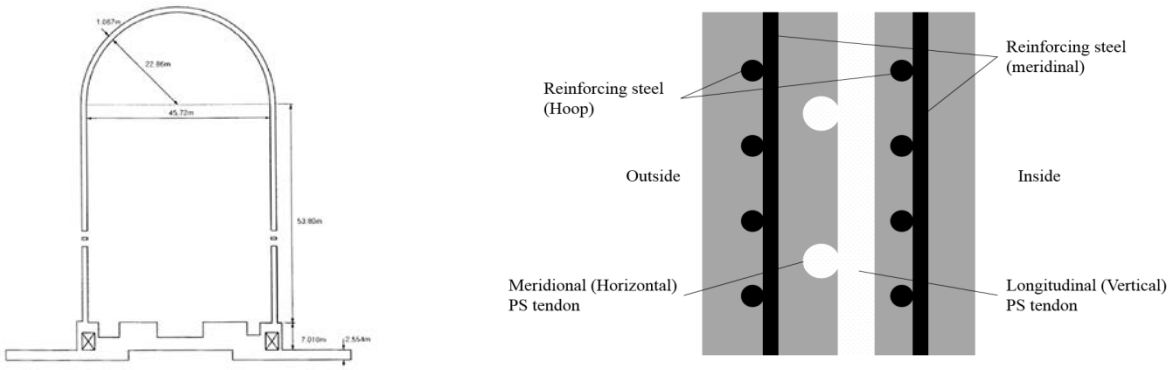

(a) PCCV dimensions (b) PCCV outer wall

Fig. 1 Details of PCCV

In this study, the quarter-thickness model was adopted for the test specimens. Therefore, the thickness of the wall is reduced to 1/4 scale of the actual size, while maintaining the other dimensions and material parameters. However, due to the reduction in the thickness, the PS force is scaled down with respect to the thickness ratio. More specifically, thickness of the specimen is 300 mm, which corresponds to 1/4 scale of the full scale outer wall thickness of 1,200 mm of the PCCV. When the top surface of the specimen (e.g., the surface directly exposed to the blast charge) is placed at the ground surface level, the blast explosion can be considered as a free explosion occurring in the atmosphere. In order to apply the full wave pressure on the specimen surface, while the charge detonates in the mid-air at 1,000 mm distance away from the loaded surface, the specimen dimensions are selected as 1,400×1,000×300 mm. This specimen size receives the explosive pressure load evenly on the top surface with minimal diffractions and interferences. Reinforcement ratio of 0.024 and the PS tendon ratio of 0.0107 are used, which are same as those used in the full scale outer wall of PCCV structure.

2.2 Blast test details

The blast experiment was conducted at the Defense Systems Test Center in the Agency for Defense Development in Korea [3]. The test specimens were prepared as shown in Table 1 for blast test. The specimen dimensions and details are shown in Fig. 2. Three types of specimens were manufactured: reinforced concrete (RC), prestressed concrete without rebar (PSC), and prestressed concrete with rebar (PSRC). For the RC specimen, D13 rebars with grid orientation were used for top and bottom reinforcements at a constant spacing of 100 mm. PS tendon used in the PSC and PSRC specimens were a 15.2 mm PS mono-strand, which can develop efficient concrete confinement from biaxial stress condition. Since the tendons used in the actual PCCVs are post-tensioned type, six strands are installed in 80 mm diameter sheath tube. Post-tensioning of the tendons is performed without grouting, making the specimen unbonded prestressed concrete. The specimen was cast using concrete with compressive strength of 40 MPa. In order to measure the structural behavior of the specimen applied with a blast load, a device capable of precisely measuring instantaneous deformations of the structure is needed. More precisely, since a blast load transmits a very strong impulse in short time duration, the measuring device has to capture the motion of the structure at instantaneous time increments. The measurement support frame used for the blast test is shown in Fig. 3. In order to expose the top surface of the specimen on the ground level with a hollow space underneath for data measurements, high-strength steel beam with 20 mm thickness is used to construct the frame to be buried in the ground. It is important to note that the frame stiffness must be stiff enough under blast loading to have no rigid body motion throughout the test. When the specimen is mounted on the frame, it is fitted firmly into the L-shaped top frame. Then, the specimen is fixed to the frame by using 8 C-clamps on four sides of the specimen. It was found that ANFO 55 lbs with 1,000 mm standoff distance was the most suitable loading setup for the test. The ANFO explosive was fixed at 1,000 mm away from the specimen using pre-manufactured square lumber hanger, as shown in Fig. 4(a), to induce a free air blast. Once the ANFO explosive was hung on the hanger, a primer-inserted subsidiary charge was installed at the center of the explosive to induce a complete explosion as shown in Fig. 4(b).

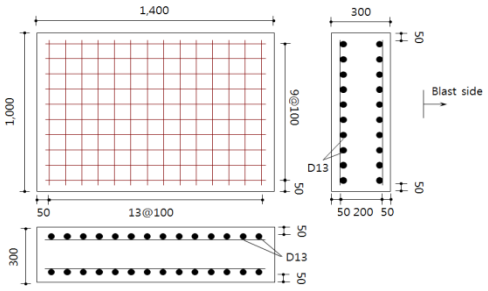

(a) RC specimen

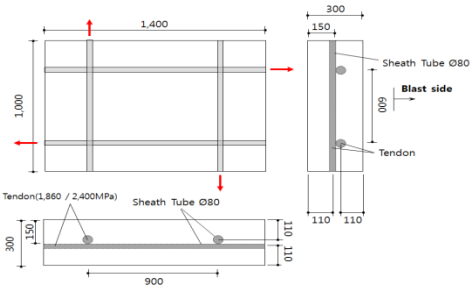

(b) PSC specimen

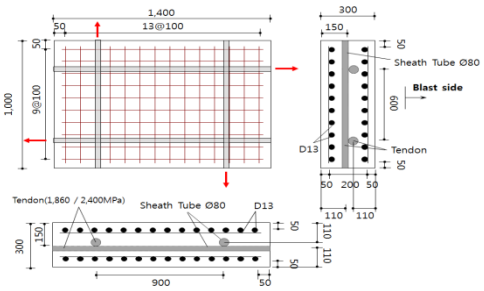

(c) PSRC specimen

Fig. 2 Specimen types and details [Unit : mm]

(a) Supporting frame

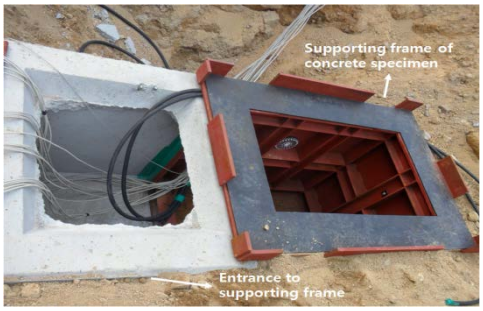

(b) Buried box supporting the specimen

Fig. 3 Support frame of panel specimen

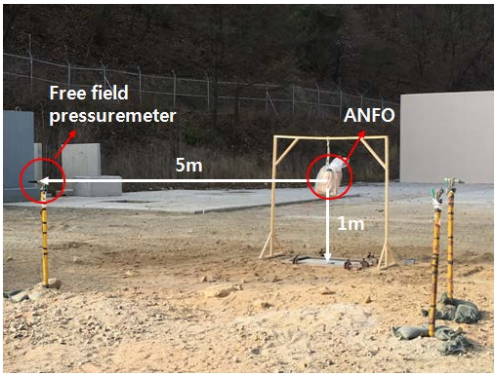

(a) Placed concrete specimen

(b) Overall explosive site

Fig. 4 Overall blast test setup and explosive charge installation

2.3 Fire test details

For the fire and blast-fire combined tests, the experiment was conducted at the Korea Institute of Civil Engineering and Building Technology (KICT) able to apply RABT fire loading. For the fire test, 10 specimens were fabricated as shown in Table 1 with 5 and 5 specimens for fire only and blast-fire combined test, respectively. As shown in Fig. 5, the fire and blast-fire combined tests were conducted using horizontal high-temperature heating furnace by applying RABT fire scenarios. In RABT fire loading curve, the temperature is raised up to 1,200 °C within 5 minutes, then the temperature is maintained at 1,200 °C for 60 minutes, followed by gradual cool down of the temperature to the room temperature for 120 minutes. Accordingly, specimens were placed in the top of the heating furnace with the blast damaged surface to be loaded by the fire. K-type thermocouples were installed during specimen fabrication at 50 mm, 100 mm, 150 mm, and 250 mm from the blast damaged surface as shown in Fig. 6 to measure the heat transfer within the concrete specimen.

Table 1. Test specimens types

Specimens		EA	Specimens		EA	Specimens		EA	Specimens		EA
Blast + residual carrying capacity			Fire + residual carrying capacity			Blast-Fire combined + residual carrying capacity			residual carrying capacity		
RC		1	RC		1	RC		1	RC		1
PSC	SWPC 7B	1	PSC	SWPC 7B	1	PSC	SWPC 7B	1	PSC	SWPC 7B	1
	SWPC 7D	1		SWPC 7D	1		SWPC 7D	1		SWPC 7D	1
PSRC	SWPC 7B	1	PSRC	SWPC 7B	1	PSRC	SWPC 7B	1	PSRC	SWPC 7B	1
	SWPC 7D	1		SWPC 7D	1		SWPC 7D	1		SWPC 7D	1
Total		5	Total		5	Total		5	Total		5
Total experiment specimens									20		

Fig. 5 Heating furnace

Fig. 6 Thermocouple location and fire specimen details

3. Blast and Fire Simulation Model

Blast and fire FEM simulations were conducted using a commercial explicit and implicit finite element program of LS-DYNA and MIDAS FEA, respectively. Simulation details used for the blast and fire simulations precisely followed those from the experiments.

3.1 Blast test details

3D model of the specimen was generated using Hypermesh 11.0 for blast analysis. 3D solid and beam elements were used to model concrete and steel rebar/PS tendon, respectively. For PS tendon modelling, an individual beam element connecting two nodal points was used. A rigid body option was used for the impactor model, because impact deformation of the impactor was much less than that of the specimen. D13 rebar and PS tendon was used in the test were modeled as a discrete beam element embedded in a 3D solid concrete element. The layout and dimensions of rebars and PS tendons were exactly as same as those of the experiment.

To uphold the panel specimen and to install measurement instrumentations underneath the specimen, steel frame was constructed. The specimen and the frame were fixed tightly using a steel edge cover and 8 C-clamps (e.g., 2 clamps on each side). In the simulations, the steel frame and the specimen was assumed to be partially fixed and partial pinned boundary condition was implemented. Therefore, the top and bottom edge nodes were given partially fixed boundary condition. The boundary between PSC specimen and ANFO was implemented using Contact Algorithm in LS-DYNA (Contact Automatic One Way Surface to Surface command) based on material model incorporating constraint effect.

3.2 Constitutive models

LS-DYNA offers many material cards to be used as its constitutive models, including concrete material models such as *MAT_BRITTLE_DAMAGE (MAT_96), *MAT_JOHNSON_HOLMQUIST_CONCRETE (MAT_111), *MAT_PSEUDO_TENSOR (MAT_16), *MAT_CONCRE TE_DAMAGE_REL3 (MAT_72), *MAT_CSCM_CONCRETE (MAT_159), etc. In this study, *MAT_CONCRETE_DAMAGE_REL3 (MAT_72R3) was used as concrete model considering damage and strain rate. MAT_072R3 can incorporate the concrete strength development factor for the dynamic strain rate based on blast loading. The reliability of the material model in predicting the response of reinforced concrete structure subjected to blast loading has been demonstrated [7]. The description of MAT_72R3 was clearly presented in the user's manual of LS-DYNA concrete-material Model 72R3 [8]. The necessary parameters are derived from compressive strength measured from 28-day compressive strength test. This study employed the model proposed in Fig. 7 for thermal characteristics of concrete such as elastic coefficient, heat expansion coefficient, and specific heat to analyze high-temperature heat transfer. Although Eurocode 2 presents thermal conductivity of concrete according to a concrete temperature within a range of 1.36-2.3 W/m°C, previous studies showed very large discrepancy between simulation results and experimental data if an existing range of thermal conductivity is used. Thus, Choi et al. (2017) proposed thermal conductivity to compensate the fire simulation model and applied this value to their fire simulations [4].

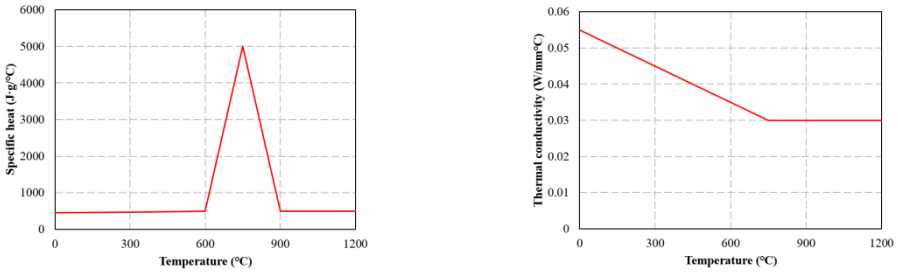

(a) Steel and tendon specific heat (b) Thermal conductivity

Fig. 7 Heat coefficient of concrete according to temperature

For rebar model, *MAT_PIECEWISE_LINEAR_PLASTICITY (MAT_24) was used. This material model takes into account isotropic and kinematic hardening plasticity. Moreover, it can define

arbitrary stress versus strain curve and arbitrary stress versus strain rate curve. For the temperature dependent specific heat and heat conductivity of steel rebar and PS tendon, the models in Fig. 8 were applied.

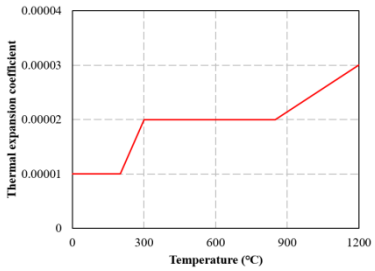

(a) Concrete thermal expansion coefficient

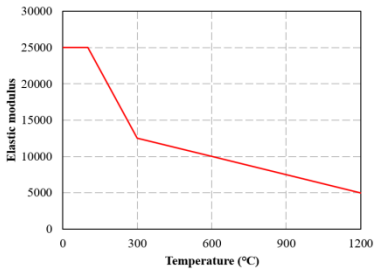

(b) Elastic modulus

Fig. 8 Thermal constitutive models

3.3 Pre-stressing force application

Pre-stressing force is applied to a concrete member by a temperature-induced shrinkage in prestressing strands. An application of pre-stressing force by the temperature induced shrinkage is recommended, because there is no direct way to apply prestressing force in structural members in an explicit FEM simulation provided by the LS-DYNA program [8]. Pre-stressing strand is typically modeled using beam element, which are constrained to concrete elements by *CONSTRAINED LARANGE IN SOLID [8]. Pre-stressing strands with a free boundary condition should contract when the temperature drops. However, when the strands are placed in concrete, the surrounding concrete restrains the contraction, giving compressive stress development in concrete. The temperature induced strain, ε_T, can be determined by the following equation (1).

$$\varepsilon_T = \Delta T \alpha \tag{1}$$

where α is the thermal expansion coefficient of strands ($\alpha = 1 \times 10^{-5}/°C$); ΔT is a temperature variation from the reference or initial temperature. The temperature change ΔT can be obtained by writing the strain compatibility equation between concrete and stands as Eq. (2):

$$\Delta T \alpha - \frac{f}{E_S A_S} = \frac{f}{E_C A_C} \tag{2}$$

where E_S and A_S are elastic modulus and cross section area of strands, respectively; E_C and A_C represents the elastic modulus and cross section area of concrete, respectively.
Given the pre-stressing force f, ΔT can be obtained by rewriting Eq. (2):

$$\Delta T = \frac{f}{E_S A_S \alpha}\left(1 + \frac{E_S A_S}{E_C A_C}\right) \tag{3}$$

It is suggested that the pre-stressing force be applied prior to performing a transient analysis in a finite element analysis program. This stress initialization process can be completed by using the DYNAMIC_RELAXATION (DR) option in the LS-DYNA software. DR is a solution method conventionally implemented to perform a quasi-static simulation in ‘pseudo’ time. The ratio of current-to-peak distortional energy (default 0.001) must be defined to achieve the convergence.

The thermal material model, *MAT_ADD_THERMAL_EXPANSION, is used for defining the temperature dependent material property for the strands. Along with this material model, the LOAD_THERMAL_LOAD_CURVE option is used for defining a temperature versus time curve. Two temperature–time curves need to be defined in this study. The first curve is for the dynamic relaxation, where the temperature is ramped up from the reference temperature to defined temperature and held steady. The second curve holds the steady-state temperature (e.g., constant temperature) for an explicit FEM simulation.

3.4 Blast load modelling

For the blast load modeling, LS-DYNA provides the *LOAD_BLAST option, which simulates blast loading on a structure. In this study, the maximum pressure from reflective pressure waves from ANFO 55lbs charge with a standoff distance of 1,000mm from the panel was used. The pressures from the blast waves were applied homogeneously to the entire top surface of the concrete panel. The time

history of blast pressure and impulse are shown in Fig. 9.

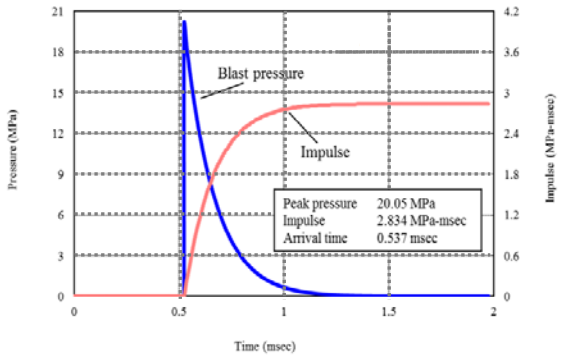

Fig. 9 Pressure-time history of ANFO 55lbs for blast simulaton

3.5 Blast induced fire simulation procedure

When fire simulation of the panels with blast damage is conducted using MIDAS FEA, the blast damage of concrete is implemented using blast simulation results obtained from LS-DYNA by elimination of concrete elements with strain exceeding allowable principal strain value of 0.01 in the panel mesh. However, the erosion criteria of the concrete elements are different for each case. Therefore, in this study, the maximum principal strain at failure is incorporated in LS-DYNA program. The element erosion failure causing maximum principal strain of concrete model was set to 0.04 based on past experimental results, which is four times the threshold value of principal strain criteria [7]. Since the spalling characteristics of RC, PSC, and PSRC specimens are different for dynamic load such as blast, the number of eliminated elements is different for the 3 panel types. Through the element elimination technique, precise and reliable fire analysis can be carried out by considering spalling damages from blast loading. The fire test results verified that the concrete surface spalling and cracking were different for the blast damaged panels compared to the panels without blast damage.

4. Model Calibrations of Blast and Fire Simulations

4.1 Blast load modelling

The maximum and residual deflection results from the blast simulations are compared to the blast test results as shown in Fig. 10. For the RC specimen, the maximum and residual deflection from the simulation was 13.29 mm and 3.64 mm, respectively. Both maximum and residual deflection between the test and simulation showed an error within 4%. For the PSC and PSRC specimens from the simulation, the maximum deflections were 7.06 mm and 8.93 mm, respectively, and the residual deflections were 2.25 mm and 2.08 mm, respectively. The PSC and PSRC specimens showed an error within 2% for the maximum deflection between the tests and simulations. However, the residual deflection had slightly larger difference between the tests and simulations in the PSC and PSRC specimens due to the differences in instantaneous prestressing force loss and recovery in the tendons. As reported in previously published study results, the maximum deflection and recovery force can vary significantly under extreme instantaneous loading characteristics such as charge shape, boundary condition, wind speed, humidity, prestressing force magnitude at the moment of blast loading. However, these factors cannot be considered in the simulation using LS-DYNA since the boundary condition, wind speed and prestressing force are constant throughout the simulation. Thus, these errors should be taken as inherent differences between the blast test and simulation. Therefore, other than these uncontrollable errors in simulation, it can be assumed that the blast simulation model is sufficiently calibrated to be used for the PCCV blast simulation.

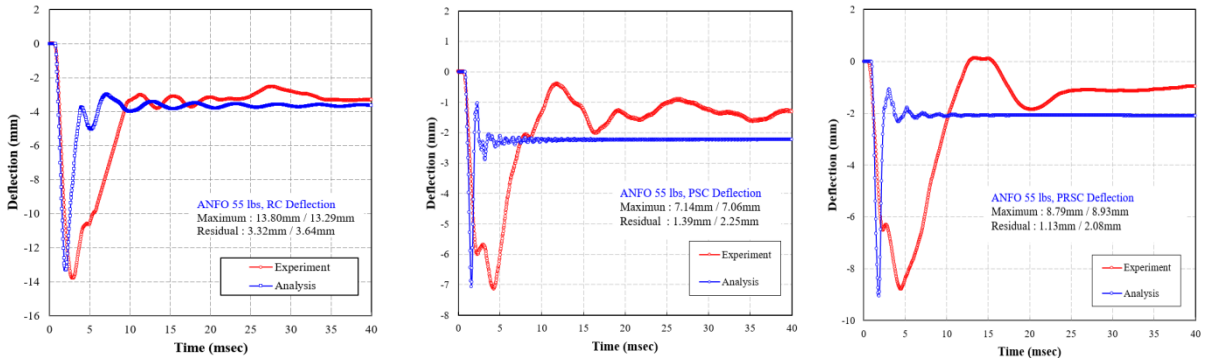

(a) RC (b) PSC (c) PSRC

Fig. 10 Comparison of blast test and simulation results

4.2 Blast induced fire model calibration

In the blast loaded specimens, the blast pressure applied surface did not experience spalling or scabbing damage as serious as expected. However, the surface had multiple macro cracks from blast loading. For fire test simulation using an implicit FEM program MIDAS FEA, blast induced cracks and craves could not be precisely implemented to the specimen model and only implemented as element eliminations from threshold plastic strain judgement. Since it cannot simulate the heat emission through the cracks found in the fire test or explosive spalling due to prestressing force, it is necessary to calibrate these results by changing the thermal material properties of concrete. The calibration was performed based on the test data by implementing different thermal coefficients with respect to the specimen depth during the modeling of PSC and PSRC specimens. Based on the study results [4], concrete thermal conductivity can increase by 1.2, 1.5, 2.0, and 2.2 times of a regular concrete thermal conductivity at the depths of 50, 100, 200, and 300 mm from the heated surface, respectively.

Fig. 11 presents the temperature distribution by location and maximum temperature with regards to blast-fire combined loading after applying the corrected thermal coefficient, respectively. In the case of the RC specimen, the temperature increased up to 1,200 °C, which showed a similar behavior to that of the RABT fire curve. The temperatures at 100 mm and 150 mm were 349.45 °C and 120.28 °C, respectively, indicating that heat did not reach the 250 mm depth. The error rate from the simulation result of the RC specimen was within 10% with the PSC specimen simulation results showing similar behavior to the RABT curve at 50 mm and 100 mm locations. A similar temperature change behavior exhibited at the 50 mm and 100 mm locations was due to explosive spalling in the test. The temperature increased to 1,200 °C up to the 100 mm location within 5 minutes after the fire loading began. The temperature at the 150 mm and 250 mm locations was 584.58 °C and 107.03 °C, respectively, with an error range within the 5% compared to that of the test results. The temperature distribution of the PSRC specimen at the 50 mm and 100 mm locations was 1,200 °C and 297.15 °C, which was similar to the experimental results. However, the temperature at the 150 mm and 250 mm location was 203.51 °C and 131.96 °C, respectively, indicating that the simulation results were 64-69 °C higher than those of the experimental results. In the fire and blast-fire simulations, factors such as explosive spalling, cracks, and internal moisture movements that occurred during fire tests were not taken into consideration. Only the thermal coefficients of concrete, rebar, and tendon were utilized, making it impossible to obtain the same results in the simulation as the test. Thus, the error range increased as the depth increased. However, since the simulation result was sufficiently accurate with regards to the blast, fire, and blast-fire test results with an error range up to 10 %, the calibrated fire simulation model can be used for real scale PCCV simulations.

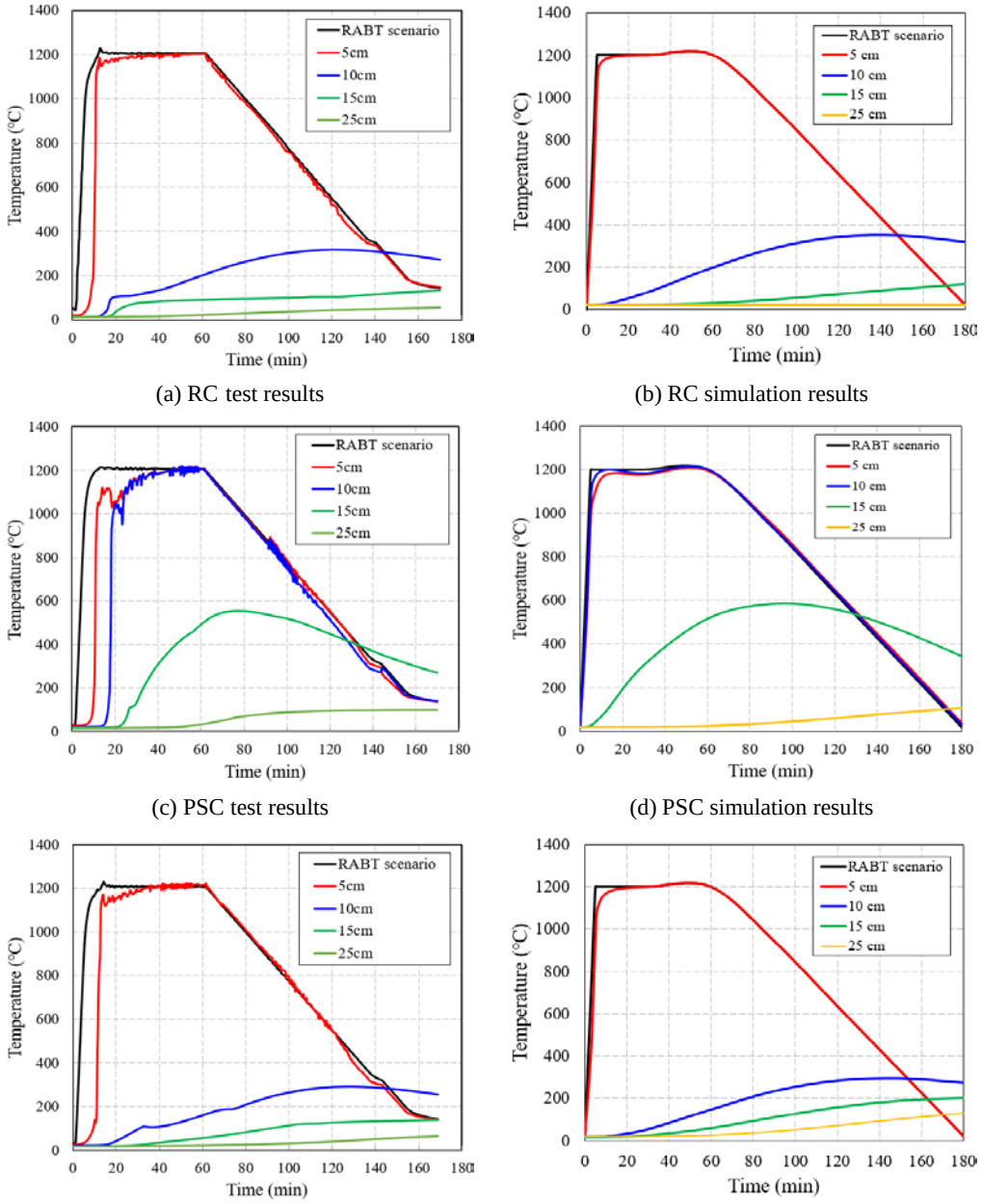

(a) RC test results (b) RC simulation results

(c) PSC test results (d) PSC simulation results

(e) PSRC test results (f) PSRC simulation results

Fig. 11 Temperature-time history curves of blast-fire test and simulation results

5. Simulations of Blast and Blast Induced Fire Loaded PCCV

5.1 Blast and fire scenarios

In order to successfully evaluate the blast resistance of PCCV, a selection of blast charge conditions that give the largest damage to a PCCV is a critical initial step. Presently, design standards are available for earthquake and impact loading conditions on PCCVs, but design standards for blast loading is still not clearly defined. Thus, an explosive charge weight and a blast standoff distance were calculated using ConWEP program and theoretical equations considering the external pressure loads for Uljin PCCV Units 1 and 2, which were designed by Flamatome Engineering Co. in France. In addition, the containment structural details of vertical and horizontal tendons and rebars are analyzed to select a blast charge detonating location of the target PCCV. From the analysis, a boundary between wall and dome is a most critical location on PCCV, which are most affected by aircraft collision and missile explosion. Based on the blast load calculation from ConWEP and the related equations, ANFO charge weight of 1,486lbs with a blast standoff distance of 5,000 mm is selected as the blast scenario as shown in Fig. 12. Blast and fire simulations are conducted on the PCCV model shown in Fig. 13. The material

models used for the simulations were as same as those used for the calibration work discussed in sections 3 and 4.

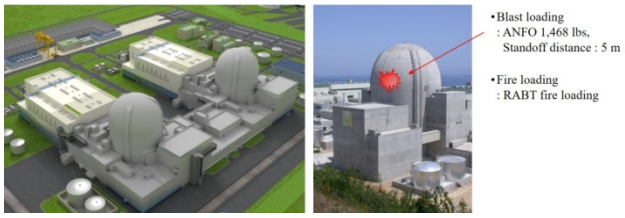

Fig. 12 Extreme loading scenarios

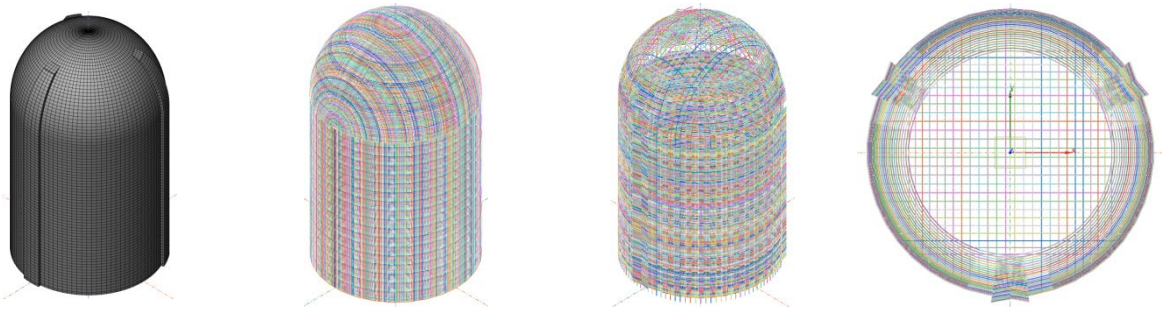

(a) Concrete model (b) Rebar model (c) Prestressing tendon model

Fig. 13 Modeling of PCCV

5.2 Blast simulation results

Comparison of the blast pressure induced by ANFO 1,486 lbs charge with 5,000 mm standoff distance calculated using LS-DYNA and ConWEP is shown in Fig. 14. The height of the joint between wall and dome in the PCCV was set as 52,730 mm for blast simulation. The peak pressure predicted in ConWEP and LS-DYNA was 4.58 and 4.46 MPa, respectively, which is a difference of 2.62 %. Although there is a slight difference in the peak pressure occurrence time between the two calculations, they are very similar in magnitude and behavior. It is important to note that ConWEP only calculates the peak pressure and does not calculate the negative reflected pressure for a charge explosion. Generally, ConWEP is used to predict the peak pressure applied to a structure in advance for preparation of blast test or simulation. Figs. 15-16 show the effective stress and deflection magnitude and behavior over time obtained at the wall-dome joint from the PCCV simulation, respectively.

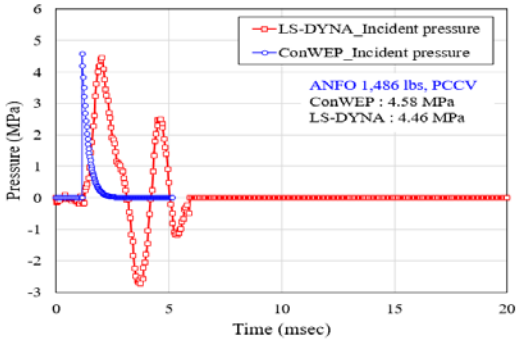

Fig. 14 Incident blast pressure of ANFO 1,486 lbs

As shown in Fig. 15, the effective stress occurrence time duration at the joint was instantaneous with 2.37 msec. The effective stress results also verified that the concentrated at the joint location directly in front of the charge, followed by gradual spreading to the area around the location until dissipation. Also, the effective stress behavior was cyclic degradation from the initial peak stress of 8.62 MPa at 2.37 msec. In Fig. 16, the deflection results of the structure increased instantaneously up to approximately 2.1 mm, followed by gradual increase up to approximately 2.7 mm and remained as plastic deflection of 2.8 mm. In contrast to the scale-down panel test results, deflection was constantly maintained near the maximum deflection due to the absence of restoring capability of prestressed tendons, because the blast

pressure was applied at the joint section with partial prestressing effect. The deflection results indirectly verified that the prestressed tendons have significant restoring effect indicated by the deflection restoration behavior shown by the blast loaded panel with bi-directional prestressing. In section 4, the principal strain threshold value is proposed as 0.04 to determine the elimination of elements to represent blast spalling effect of concrete. However, the maximum principal strain calculated from LS-DYNA was 0.039 when 1,486lbs ANFO charge detonating at a 5,000 mm standoff distance is applied. Therefore, concrete elements were not eliminated, because the strain did not exceed 0.04.

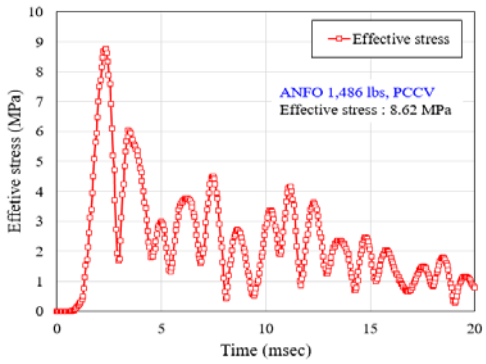

Fig. 15 Effective stress of of PCCV

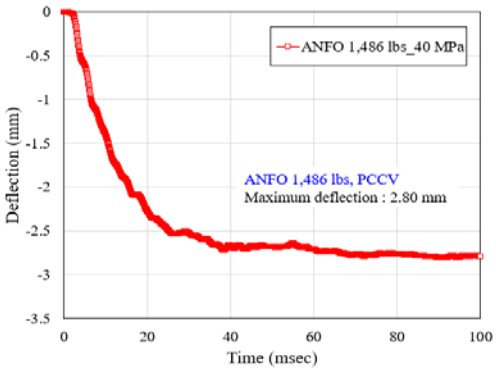

Fig. 16 Time-deflection history curve of PCCV

5.3 Blast induced fire simulation results

The fire scenario was selected in which the fire occurred instantaneously following the blast load. The fire analysis of PCCV under blast-fire combined loading according to RABT scenario. Since the maximum principal strain of concrete did not exceed 0.04, the elements were not eliminated, assuming that no concrete failure occurred at all. However, the panel experiment in section 2 showed that even though the concrete member damaged by the blast load did not have exfoliation or local damage, a large number of cracks were generated. Thus, simulations and calibrations were conducted in section 4 by increasing the thermal conductivity of the concrete considering the cracks, which is also used in PCCV simulations by increasing thermal conductivity.

To verify the temperature transfer trend in the wall from the blast-fire combined loading, the comparison of the temperature distribution results in the wall from the simulations are shown in Fig. 17. Fig. 17 shows the temperature distribution at various depths of the wall (i.e., 0, 200, 400, 600, 800, 1,000, and 1,200 mm) and the maximum temperature at the boundary between the wall and the dome. The surface temperature of the concrete where the RABT fire occurred showed the same trend as the fire curve. The temperature at 200 mm depth was 375.75 °C and the temperatures at 400 mm or deeper depths exhibited temperatures of less than 200 °C. The temperature at the internal surface of the wall was 21.01 °C, demonstrating no heat reached the depth. The temperature of the dome at 200 mm depth was 331.98 °C, which was around 88% of that at the joint, and the temperature continued to decrease in the same manner at the greater depths. The temperature in the wall at 200 mm depth was 362.49 °C, which was higher than that at the dome and approximately 96 % of that at the joint.

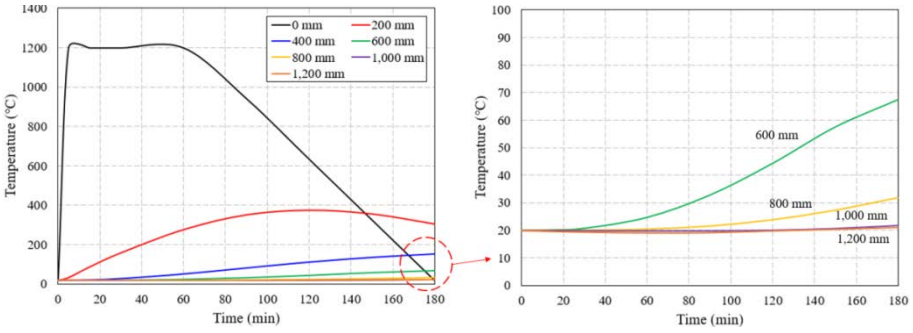

Fig. 17 Time-temperature history curve of PCCV wall

6. Parametric Study of Blast Induced Fire Loaded PCCV

6.1 Parameter selections

This section discusses about parametric study results using the PCCV simulation models discussed in previous sections. The selected parameters include standoff distance, charge weight, and concrete compressive strength. As presented in Table 11, the standoff distance of 1,000, 3,000, and 5,000 mm for 1,486 lbs of charge weight was used for the simulations. As presented in Table 12, the explosive charge weight and the concrete compressive strength of 1,486, 4,458, and 7,430 lbs and 40, 50, and 60 MPa, respectively, were used for the simulations. After the blast simulation, the fire simulation was conducted to obtain the temperatures at various depths.

6.2 Parametric study results

The compressive strength and charge weight parametric study results from the blast simulations are shown in Fig. 18 and Table 2. For 1,486 lbs of ANFO charge weight, the maximum deflections using concrete compressive strength of 40, 50, and 60 MPa were 2.80 mm, 2.79 mm, and 2.72 mm, respectively, indicating that the blast resistance increased as the compressive strength increased. Also, as the blast load increased by increasing the charge weight from 4,458 lbs to 7,430 lbs, the maximum deflection increased. However, when the concrete compressive strength increased, the deflection slightly decreased. Based on the maximum principal strain of 0.04, the parametric study results showed that the damage volume of all the specimens of 40, 50, and 60 MPa was 0.0 mm^3 when the charge weight of 1,486 lbs was applied as shown in Tables 3-4. From the charge weight of 4,458 lbs or more, the damage volume increased proportional to the increased charge weight and concrete compressive strength.

Table 2. Simulation results of standoff distance variation

Concrete compressive strength	Explosive charge weight	Value	Standoff distance		
			1 m	3 m	5 m
40 MPa	1,486 lbs	Max. Deflection (mm)	65.79	8.71	2.80
		Damage volume (mm^3)	$9{,}864 \times 10^6$	0	0
		Max. principal strain	0.0412	0.0138	0.0114

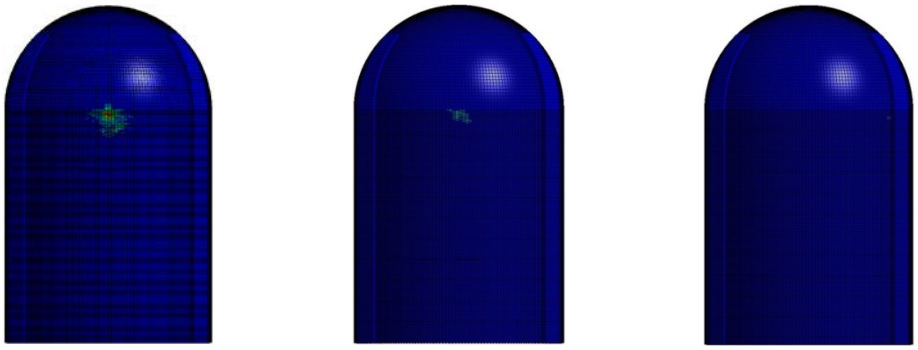

(a) 1,000 mm (b) 3,000 mm (c) 5,000 mm

Fig. 18 Maximum principal strain of standoff distance variation on PCCV

The compressive strength and charge weight parametric study results from the blast simulations are shown in Table 3. For 1,486 lbs of ANFO charge weight, the maximum deflections using concrete compressive strength of 40, 50, and 60 MPa were 2.80 mm, 2.79 mm, and 2.72 mm, respectively, indicating that the blast resistance increased as the compressive strength increased. Also, as the blast load increased by increasing the charge weight from 4,458 lbs to 7,430 lbs, the maximum deflection increased. However, when the concrete compressive strength increased, the deflection slightly decreased. Based on the maximum principal strain of 0.04, the parametric study results showed that the

damage volume of all the specimens of 40, 50, and 60 MPa was 0.0 mm^3 when the charge weight of 1,486 lbs was applied as shown in Tables 3-4. From the charge weight of 4,458 lbs or more, the damage volume increased proportional to the increased charge weight and concrete compressive strength.

Table 3. Blast simulation results of compressive strength and charge weight variations

Concrete compressive strength	Value	Explosive charge weight		
		1,486 lbs	4,458 lbs	7,430 lbs
40 MPa	Max. Deflection (mm)	2.80	5.38	8.92
	Damage volume (mm^3)	0	$4{,}932 \times 10^6$	$12{,}604 \times 10^6$
50 MPa	Max. Deflection (mm)	2.79	5.31	8.71
	Damage volume (mm^3)	0	$3{,}548 \times 10^6$	$8{,}768 \times 10^6$
60 MPa	Max. Deflection (mm)	2.72	4.57	8.33
	Damage volume (mm^3)	0	$2{,}740 \times 10^6$	$4{,}288 \times 10^6$

Table 4. Maximum principal strain results of compressive strength and charge weight variations

Concrete compressive strength	Explosive charge weight		
	1,486 lbs	4,458 lbs	7,430 lbs
40 MPa	0.0114	0.307	1.08
50 MPa	0.0028	0.0447	0.207
60 MPa	0.00075	0.0128	0.0887

The blast-fire combined simulation results according to the standoff distance are presented in Table 5. The fire simulation was conducted by applying the fire load to the area damaged by the blast load. As stated previously, no elements with the principle strain exceeding 0.04 were found in the PCCV applied with the blast load at 3,000 and 5,000 mm standoff distance. Therefore, the blast-fire simulation results from the standoff distance parametric study results were same. However, the blast-fire simulation results at 1,000 mm standoff distance showed that the concrete temperature at 200 mm depth from the outer surface was 372.77 °C, which was approximately 2.98 °C lower than the temperature of 375.75 °C obtained from the simulations at 3,000 and 5,000 mm standoff distance. At 600 mm depth from the outer surface, the combined blast-fire loaded specimen at 1,000 mm standoff distance exhibited a lower temperature than that from the simulations using 3,000 and 5,000 mm standoff distance. However, at 800 mm depth, the temperature obtained from 1,000 mm standoff distance was approximately 1 °C higher than that obtained from 3,000 and 5,000 mm standoff distance. The temperature difference was due to the element eliminations from blast loading, which directly exposed the internal wall elements to the fire temperature as shown in the result summary of Table 6.

Table 5. Temperature distribution of standoff distance variation [Unit : °C]

Concrete compressive strength	Explosive charge weight	Depth	Standoff distance		
			1 m	3 m	5 m
40 MPa	1,486 lbs	200 mm	372.77	375.75	375.75
		400 mm	144.36	153.82	153.82
		600 mm	52.55	67.54	67.54
		800 mm	32.30	31.89	31.89

Table 6. Temperature distribution of compressive strength and charge weight variations [Unit : °C]

Concrete compressive strength	Depth	Explosive charge weight		
		1,486 lbs	4,458 lbs	7,430 lbs
40 MPa	200 mm	375.75	370.90	369.82
	400 mm	153.82	152.28	151.96
	600 mm	67.54	47.76	45.71
	800 mm	31.89	35.61	36.61
50 MPa	200 mm	412.21	409.17	376.80
	400 mm	177.95	176.96	174.51

	600 mm	70.53	65.09	64.55
	800 mm	31.87	35.39	39.26
60 MPa	200 mm	442.54	442.52	442.14
	400 mm	202.20	202.05	201.01
	600 mm	86.12	86.31	87.57
	800 mm	37.79	37.80	38.52

6. Conclusions

In this study, the extreme loading capacities and behaviors of PCCV structure under blast, fire and blast-fire combined loading were evaluated. The bi-directional prestressed concrete panel members were experimentally evaluated and analytically verified using commercial finite element programs. Finally, a damage level was evaluated for a full-scale PCCV structure for extreme loading. The conclusions obtained in this study are as follows:

(1) In this study, the blast-fire combined test obtain accurate data using the scale-down model tests for the walls applied to actual PCCV structure, and the data increase the reliability of the precision analysis results using finite element programs and calibrating the results.

(2) The calibrated simulation tools can be used for full-scale PCCV precision simulations under extreme combined loading scenarios, such as blast and fire. The simulation results showed that no significant damage occurred under the blast-fire scenario with a standoff distance of 5,000 mm, and ANFO charge of 1,486lbs with RABT fire load. Under the fire load, the structure was affected around the blast damaged area, but no significant damage affecting the rest of the structure was observed. The study results imply that damage to actual PSC structures can be predicted numerically using the verified simulation model in blast induced fire accident scenarios.

(3) The parametric study was conducted according to the explosive charge weight, standoff distance, and concrete compressive strength of the PCCV structure using blast and fire simulation tools calibrated by the test data. Based on the study results, the level of damage to full-scale structures can be evaluated by applying various blast-fire scenarios and parameters.

Acknowledgements

This work was supported by the National Research Foundation of Korea(NRF) grant funded by the Korean government(MSIT:Ministry of Science and ICT) (No. 2017M2A8A4056624)

References

[1] Hyde, D.W., *Fundamental of protective design for conventional weapons, CONWEP (conventional weapons effects). TM5-8511-1,* 1992.

[2] Krauthammer, T., *Blast-resistant structural concrete and steel connections*, International Journal of Impact Engineering, Vol.22, No.9-10, pp.887-910, 1999.

[3] Choi, J.H., Choi, S.J., Cho, C.M., Kim, T.K., and Kim, J.H.J., *Experimental Evaluation of Bi-directionally Unbonded Prestressed Concrete Panel Blast Resistance Behavior under Blast Loading Scenario,* Journal of the Korea Concrete Institute, Vol.28, No.6, pp.673-683, 2016.

[4] Choi, S.J., Lee, S.W., Kim, and J.H.J., *Impact or blast induced fire simulation of bi-directional PSC panel considering concrete confinement and spalling effect,* Engineering Structures, Vol.149, pp.113-130, 2017.

[5] Ross, C.A., Purcell, M.R., and Jerome, E.L., *Blast response of concrete beams and slabs externally reinforced with fibre reinforced plastics (FRP).* Proc. of the Congress. XV-building to last, pp.673-677, 1997.

[6] Muszynski, L.C., and Purcell, M.R., *Use of composite reinforcement to strengthen concrete and air-enterained concrete masonry walls against air blast,* Journal of composites for construction, Vol.7, No.2, pp 98-108, 2003.

[7] Jiang, H., and Chorzepa, M.G., *An effective numerical simulation methodology to predict the impact response of pre-stressed concrete members,* Engineering Failure Analysis, Vol.55, pp.63-78, 2015.

[8] LSTC (Liverore Software Technology Corporation)., *LS-DYNA Keyword User's Manual*, Version 971, 2007.